Rotor-Speed Stability Improvement of Dual Stator-Winding Induction Generator-Based Wind Farms By Control-Windings Voltage Oriented Control

Mohammad Hassan Zamani, Gholam Hossein Riahy, and Mehrdad Abedi

***Abstract*—This paper studies the rotor-speed stability improvement of dual stator-windings induction generator (DWIG)-based wind farms under power system fault conditions. The characteristics of the DWIG-based wind turbines are described. The factors affecting the rotor-speed stability are analyzed, and a novel control-winding voltage oriented drive together with braking resistor (BR) is proposed to control both the active and the reactive power of DWIG during the fault. The proposed control method provides additional supplementary control loop to conventional control-winding voltage oriented drive. The supplementary control loop devoted to adjust the BR value in such a way that the whole kinetic energy of generator and turbine is absorbed by BR. Additionally, the orientation of control winding voltage forces the slip of DWIG to be approximately constant; thereby, limiting the reactive power consumption during the fault. The simulation and experimental works from the prototype of 1.2-kW three/three-phase DWIG wind power system demonstrate the effectiveness of the control scheme as also the significant influence of BR for improving the rotor-speed stability of DWIGs.**

***Index Terms*—Braking resistor (BR), dual stator-winding induction generators (DWIG), offshore wind farm, rotor-speed stability, voltage oriented control.**

I. Introduction

In recent years, due to the fast consumption of fossil fuels and the increasing environmental concerns, wind energy, as one of the most widely utilized renewable resources, has been attracting more and more attentions. Although the majority of wind turbines is situated on land, there is a growing demand for wind turbines to be placed offshore, where wind conditions are generally better, and the issues of the noise and the impact on the landscape are somewhat ameliorated [1]. A common problem to all offshore energy conversion systems is the electrical cable connection to the onshore substation. This must be by a buried undersea cable and this then raises distance issues because all ac cables have high capacitance and the line charging current for long cable runs can be very high. Therefore, the use of high-voltage dc (HVdc) technology is one of the prospective solutions for large offshore wind farms [2].

Dual stator-windings induction generator (DWIG) exhibits strong coordination by HVdc transmission, and would, therefore, be an attractive and economical candidate for large offshore wind farms with HVdc transmission [3]. In these generators, there are two sets of windings in the stator slots. One, referred to as a power winding with a diode bridge rectifier may feed directly into the HVdc link, and the other, called excitation or control winding, is connected to a voltage source converter and provides a supply of the reactive power in order to produce the magnetizing flux in the DWIG [4]. For aircrafts and ships applications, the dual construction has the advantage of effectively regulating of the voltage magnitude and load frequency, while minimizing or eliminating converter-induced harmonics in the load with a possibility of increasing the output power and optimizing system efficiency [5] and [6]. Also, the DWIG has many other advantages, such as innate brushless construction, low-maintenance demand, wide speed range, and good performance of the dc voltage output with a small-size power converter under the variations of speed and load. This shows that DWIGs can also be used in wind power systems, especially as a potential solution for the offshore wind farms using the HVdc transmission.

In 2011, a 6/3-phase DWIG was proposed as an economical variable-speed solution to operate as a wind turbine generator of offshore wind farm with HVdc transmission [3]. In 2015, to further widen the speed rang of DWIG based-wind turbines and maximum power point tracking, the dc bus on the power-winding side is connected in parallel and a wide-speed-range-operation DWIG system with control-winding-flux-orientation control strategy is proposed [7]. Although, DWIG integration into the HVdc transmission may seem a suitable alternative for offshore wind farm application, they must be taken into account in the various aspects of network analyses, to ensure safe and reliable operation of offshore wind farm.

One of the major problems related to the all wind turbine technologies, irrespective of type employed in wind farms, is rotor-speed stability. It is well known that faults which occur on the transmission lines may cause a significant speed increase of the turbine and generator rotor. After the fault clearance, the rotor speed of the wind turbine may be so high that it does not return to a stable value [8].

This paper identifies and analyses the nature of transient stability of DWIGs and proposes a method for enhancing

Manuscript received June 28, 2015; revised September 20, 2015; accepted October 19, 2015. Date of publication October 28, 2015; date of current version March 2, 2016. Recommended for publication by Associate Editor M. Molinas.

The authors are with the Wind Energy Laboratory, Electrical Engineering Department, Amirkabir University of Technology, Tehran 15875-4413, Iran (e-mail: mhz102@aut.ac.ir; ghoam@aut.ac.ir; abedi@aut.ac.ir).

Color versions of one or more of the figures in this paper are available online at http://ieeexplore.ieee.org.

Digital Object Identifier 10.1109/TPEL.2015.2495256

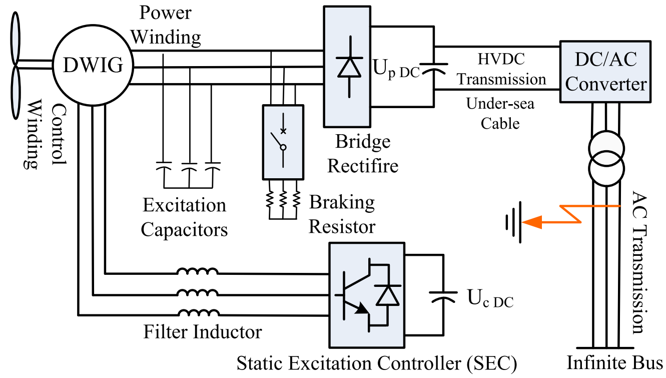

Fig. 1. Schematic diagram of a grid-connected DWIG-base wind turbine which is subjected to a tree-phase fault from the power winding side.

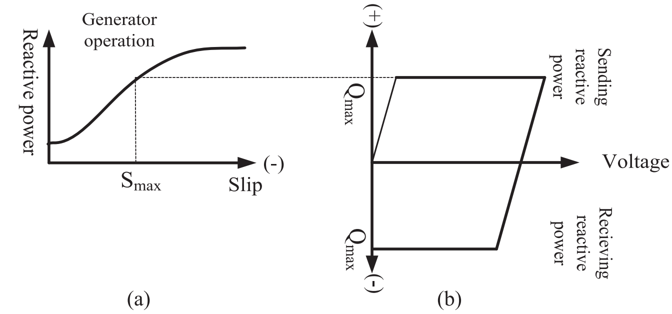

Fig. 2. Reactive power-slip curve of a DWIG and the operating area of its SEC disturbance.

rotor-speed stability of DWIGs. For a synchronous generator-based wind farm, the problem of rotor-speed instability is due to the lack of output active power. For a wind farm based on induction generators, the main problem is reactive power. The system instability of this wind farms is largely caused by the excessive reactive power absorption by induction generator after fault due to the large rotor slip gained during fault [9], but for a DWIG-based wind farm, both the lack active power and the high reactive power demand pose a serious threat to rotor-speed stability. A novel control-winding voltage oriented control together with braking resistor (BR) is proposed to overcome the instability problem. The control-winding voltage oriented control is highly robust with respect to the change in machine parameters [10]. In addition, by this control method, the slip of DWIG could be kept close to its nominal value, minimizing reactive power absorption by DWIG during the fault. The BR is also proposed to control the rotor speed during the fault when the kinetic energy of the wind turbine continuous to increases because of rotor acceleration [11]. The BR is connected to the power winding of DWIG, absorbing excessive energy carried in the wind that cannot be transferred to the power system.

II. System Stability of DWIG-Based Wind Turbines

The system configuration of a DWIG-based offshore wind turbine is shown in Fig. 1. The DWIG is connected to the mainland grid via a HVdc transmission. The output of DWIG, i.e., the power winding, feeds its electrical power into the HVdc link via a diode rectifire. The HVdc transmission system is connect to the ac transmission network through a dc/ac convertor and a step-up power transformer. The fault is assumed to occur on ac transmission line near the power transformer. A fixed excitation capacitor bank is connected across the terminal of the power winding to provide significant proportion of the total reactive power consumption. On the control-winding side, the static excitation capacitor (SEC) is connected to produce variable reactive power, through which the regulation of the reactive power in different working conditions is achieved. A dc-bus capacitor is used as a voltage source $U_{c\,\mathrm{DC}}$ to the SEC. The SEC is connected to control winding via a filter inductor to reduce the high-frequency harmonics injected into the machine, thereby reducing output voltage harmonics of the machine [12].

During the fault in the power system, DWIG with control-winding oriented voltage control has three advantages over conventional induction generators which are as follows.

1) The conventional induction generators are directly connected to power system, and when the fault occurs, the voltage at the terminals of the generator drops significantly, causing the electromagnetic torque and electric-power output of the generator to be greatly reduced. However, the mechanical-input torque is almost constant during typical nonpermanent faults and this causes the machine to accelerate. The frequency of the power system is constant and acceleration of generator causes the slip of generator to increase [13]. Fig. 2(a) shows how the reactive power consumption by induction generator increases as slip increases so that when the fault cleared, these generators draw a large amount of reactive power from the system.

For wind turbine based on squirrel-cage induction, after a severe fault occurrence, the squirrel-cage induction generator can reach reactive power consumption up to twice its rated power. If this is not available, the generator continues to accelerate, and this may lead to rotor-speed instability [9]. This problem may also threaten the rotor-speed stability of the DWIG-based wind farm. During the fault, if the slip of the DWIG is not properly limited then the SEC of DWIG is not able to provide the enough reactive power to DWIG. In practice, for a DWIG, the maximum capacity of SEC is about 35% of the rated output power and such a SEC is not able to fully generate the reactive power of DWIG without controlling the slip [3]. Fig. 2(b) shows the operating area of the SEC. It has been assumed in this figure that the SEC generates (absorbs) maximum reactive power of $Q_{\max}$.

As shown in this figure, in case of severe disturbance in the power system, if the fault was on for a long period and not cleared until the slip exceeds the critical value $S_{\max}$, the SEC will not be able to generate required reactive power of the DWIG. In such situation, a further increase in slip may threaten the operation of DWIG system. This may cause worsening of the reactive power balance, leading to decrease in the flux and electric torque of DWIG, so that according to (1), may lead to rotor-speed instability

$$T_m - T_e = j \cdot \frac{d\omega}{dt}. \tag{1}$$

Fortunately, the DWIG has good slip-control capability due to the possibility of controlling the frequency of control-winding voltage. The SEC of control winding allows full control of frequency, and, therefore, synchronous speed of the DWIG. Controlling the frequency of the control winding will make it possible to keep the synchronous speed of DWIG close to the rotor speed, minimizing the slip, and, therefore, the reactive power of the DWIG. As a control drive strategy, control-winding oriented control is selected to achieve both a quick response and limiting of the changes in slip. In this drive strategy, putting all of the control-winding voltage in the *d*-axes makes it possible to control both the electric torque and the reactive power of the SEC [10]. Also, the frequency of the control-winding voltage is chosen in such a way that a constant-slip operation of DWIG is obtained.

2) The second advantage related to rotor-speed stability of DWIG is that the active power compensators like BR is capable of absorbing its nominal active power during the disturbance. Also, the fixed capacitor bank is able to generate its nominal reactive power. The BR is a resistor with a very high-power dissipation capacity for short time periods. It can be viewed as a fast load injection to absorb the excess transient energy caused by a disturbance. The brake is shunted between the terminals of the generator and earth to dissipate the excess energy gained by the generator during the transient period [11] and [14]. The absorbed electrical power by the BR is proportional to the square of the voltage. For conventional induction generators, the terminal voltage drop significantly during the fault. Therefore, the BR has not a considerable effect on improving transient stability of the conv entional induction generator, but in contrast to the conventional induction generators (i.e., squirrel cage and wound-rotor induction generators), the transient stability of a DWIG would be significantly improved by using the BR. The power and control windings have no electrical connection. Therefore, the fault which occurs in the power winding side, do not strongly affect the operation of control winding that is responsible for providing the reactive power and for regulating the output voltage of the power winding. One special feature of this arrangement is that the SEC of DWIG always ensures the magnetic field is active so that it will always induce an emf in the power windings. In other words, from the reactive power point of view, the DWIGs are similar to the synchronous generators in which the dc excitation winding ensures the reactive power and output voltage all the time. During the fault, if the power winding side of the DWIG is disconnected from the HVdc transmission, then the voltage of power winding will not depress, so maintaining the voltage of power winding. In this situation, the BR has as large an influence as possible, and the maximum improvement in rotor-speed stability will be obtained. Furthermore, during the fault, as the terminal voltage of both the power winding and the control winding remain constant, the fixed capacitor bank of the DWIG is able to generate its nominal reactive power. For conventional induction generators, the terminal voltage of generator drops significantly during the fault so the fixed capacitor bank is incapable of generating any reactive power.

3) In addition to these two advantages, the DWIG with control-winding voltage oriented control has another important property that must be taken in to account. During the fault, by increasing the rotor speed of DWIG, the control-winding voltage oriented control increases the frequency of SEC, decreasing the reactance of fixed excitation capacitor bank $\frac{1}{2\pi fc}$ which is connected across the terminal of the power winding. As mentioned before, during the fault, the voltage of power winding remains constant. Therefore, a linear relationship between the rotor speed and reactive power generated by fixed capacitor bank can be assumed. The more the acceleration of DWIG, the more reactive power generated by capacitor bank and the less reactive power generated by SEC [12]. This feature can be taken advantage of because, this prevents the SEC to overload $Q_{\max}$ and avoid disturbing the reactive power balance of the DWIG.

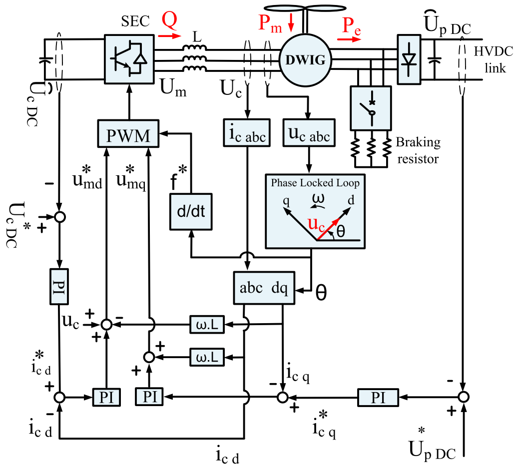

Fig. 3. Control-winding oriented control of the HVdc-connected DWIG.

III. Control-Winding Voltage Oriented Control of DWIG

Fig. 3 shows a DWIG based-wind turbine with control-winding voltage oriented control. This DWIG is also equipped with BR.

The DWIG is connected to the ac system via a HVdc transmission. The control system employs decoupling control strategy with pulse width modulation. According to the instantaneous power theory, active power and reactive power of the control winding can be expressed as [15]:

$$P_c = \boldsymbol{U}_c \cdot \boldsymbol{I}_c = u_{cd} \cdot i_{cd} + u_{cq} \cdot i_{cq} \tag{2}$$

$$q_c = \boldsymbol{I}_c \times \boldsymbol{U}_c = u_{cq} \cdot i_{cd} - u_{cd} \cdot i_{cq} \tag{3}$$

where P_c is the active power and q_c is the reactive power; $\boldsymbol{I}_c$ is the current vector of the control winding; i_{cd} and i_{cq} are the *dq* components of control winding current i_c. Using phase-locked loop and putting all of the control-winding voltage in the *d*-axes,

$u_{cq} = 0$, it is clear that

$$P_c = u_{cd} \cdot i_{cd} = \omega_1 \cdot \psi_c \cdot i_{cd} \tag{4}$$

$$q_c = -u_{cd} \cdot i_{cq} = \omega_1 \cdot \psi_c \cdot i_{cq}. \tag{5}$$

In these equations, ω_1 is the angular stator electrical frequency. These equations show that i_{cq} produces the instantaneous reactive power q_c, while i_{cd} generates the P_c, namely

$$i_c \xrightarrow{U_c-\text{oriented}, U_c = u_{cd}} \begin{cases} i_{cd} & \Rightarrow & P_c \\ i_{cq} & \Rightarrow & q_c. \end{cases} \tag{6}$$

The q_c can regulate the control winding flux at different speed and load. Also by regulating P_c, the electrical torque T_{emc} of SEC can be regulated. For a DWIG, any change of control-winding flux ψ_c will cause the variation of air-gap flux and lead to the regulation of $U_{P\,\mathrm{DC}}$. In addition, the dc-bus voltage of control winding $U_{c\,\mathrm{DC}}$ must be under control to ensure the normal work of SEC, which can be implemented by the regulation of the electromagnetic torque of control winding T_{emc}. Therefore, the control mechanism for the DWIG system under variable rotor speed and different load for the wind power application is written as follows:

$$i_c \xrightarrow{U_c-\text{oriented}} \begin{cases} i_{cd} & \Rightarrow & P_c & \Rightarrow & T_{emc} & \Rightarrow & U_{c\,\mathrm{DC}} \\ i_{cq} & \Rightarrow & q_c & \Rightarrow & \psi_c & \Rightarrow & U_{P\,\mathrm{DC}}. \end{cases} \tag{7}$$

For a DWIG with control-winding voltage oriented control, $u_{cq} = 0$ and $U_c = u_{cd}$, so according to the Kirchhoff law and Fig. 3, the voltage equation can be yielded as follows:

$$\begin{bmatrix} U_{md} \\ U_{mq} \end{bmatrix} = L\frac{d}{dt}\begin{bmatrix} i_{cd} \\ i_{cq} \end{bmatrix} + L \cdot \omega_1 \cdot \begin{bmatrix} -i_{cq} \\ i_{cd} \end{bmatrix} + \begin{bmatrix} U_c \\ 0 \end{bmatrix} \tag{8}$$

and, therefore, for a DWIG with decoupling control strategy

$$\begin{bmatrix} U^*_{md} \\ U^*_{mq} \end{bmatrix} = \begin{bmatrix} PI(i_{cd}, i^*_{cd}) \\ PI(i_{cq}, i^*_{cq}) \end{bmatrix} + L \cdot \omega_1 \cdot \begin{bmatrix} -i_{cq} \\ i_{cd} \end{bmatrix} + \begin{bmatrix} U_c \\ 0 \end{bmatrix}. \tag{9}$$

The above consideration lead to the conclusion that control-winding voltage oriented control not only has no direct relation with machine parameters [10], as discussed in [16], but also the need of stator flux observer, speed estimation, and flux oriented algorithm are eliminated. The detailed description of the stator-voltage oriented control can be found in [3] and [10].

IV. Control-Winding Oriented Control With Supplementary Control Loop

For stable operation of DWIGs in wind power applications, besides controlling the active power and the reactive power of SEC (control winding), the power balance between the electrical power transmitted to HVdc and the mechanical power delivered by the wind turbine must be held. The imbalance power of wind turbine-based DWIG will cause unexpected changes in rotor speed. Therefore, any further difference between electrical output power (power winding) and mechanical input power (wind power) causes either rotor-speed instability or stop the turbine. On other words, for stable operation of DWIG, the amount of output power of DWIG must be forced to have precisely the same value of mechanical input power of wind turbine (neglecting the losses). During the steady state, the balance of active power can be achieved by coordinate control of wind turbine and HVdc transmission.

However, during the fault, the protective equipment disconnects the HVdc transmission from the faulty ac system then no electric power will be allowed to transmit from wind turbine. Therefore, the only way for preventing rotor-speed instability following a large disturbance is to employ BR. The power in the wind varies quite rapidly and unpredictably, so that the amount of BR must be changed instantaneously depending on the wind speed condition. At any moment during the disturbance, the amount of active power of BR must be forced to have precisely the same value of active power of DWIG. Yuwen *et al.* [17] explain how the dc-bus voltage of control windings is also strongly affected by the difference between the mechanical input power (wind power) and output power (BR power and losses). Therefore, an additional supplementary control loop must be added to control-winding voltage oriented drive to obtain fast and accurate active power balance of DWIG during the fault. Similar to static VAR compensator SVC in which the reactive power control can be accomplished by controlling the value of capacitive suseptance, the active power balance of standalone DWIG can be performed by controlling the value of BR. The BR can be considered as an active shunt element, and, therefore, the control strategy for SVC can also be applied for controlling the BRs. A comprehensive explanation of this control method can be found in [18]. This arrangement is an expensive system with high rating current of thyristor switches. Also, this control scheme is slow acting system and the rate of change of BR is limited to typically 20 ms (one cycle of DWIG frequency).

To overcome these problems, in this paper, a new supplementary control loop for controlling the power of BR is proposed. The combination of this power-control loop and control-winding voltage oriented drive provides a novel drive strategy which is useful to fault condition. Also, this control method is applicable for the standalone application of DWIG based-wind turbine. Fig. 4 shows the schematic diagram of this control strategy. The switch S is a SCR with auxiliary turn-off circuitry. This switch is controlled by the output of the comparator. The duty cycle control signal may vary between zero and one, $0 \leq k \leq 1$. When k is greater than the ramp signal, S is closed and the diode D is ON. Therefore, the BR gives the minimum value of *R*. This corresponds to time interval t_1 in Fig. 4. When k is less than ramp signal, the logic output is low, S is opened and diode D is OFF. Therefore, the BR gives the maximum value of *(n+1).R*. This corresponds to time interval t_2 in Fig. 4. Therefore, this supplementary control loop is able to adjust the value of BR between *R* and *(n+1).R* during the fault. The amount of active power of BR can be varied between $3. \frac{E_s^2}{(n+1)\cdot R_{\mathrm{BR}}}$ and $3 \cdot \frac{E_s^2}{R_{\mathrm{BR}}}$. It is worth noting that the dynamic response of the system could be increased by increasing the frequency of repeating sequence wave.

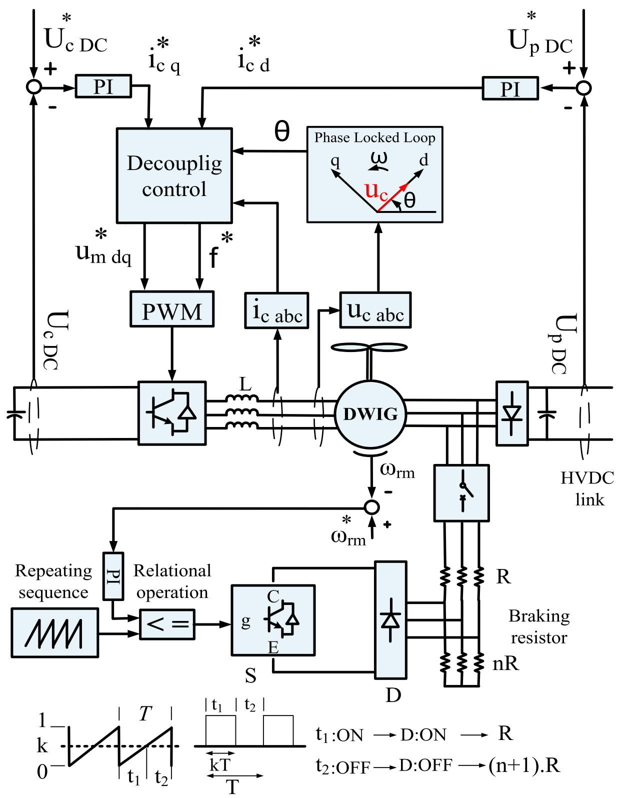

Fig. 4. Novel control-winding oriented drive for coordinate control of a DWIG and BR.

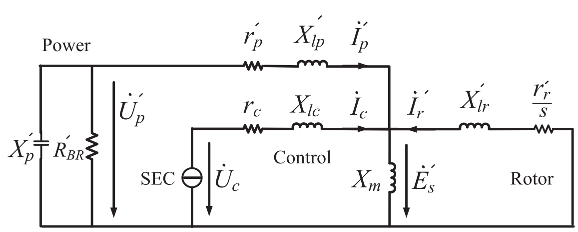

Fig. 5. Reactive power-slip curve of a DWIG.

The remaining question is the determination of allowable value of BR for stable operation of DWIG during the fault. The DWIG can be represented by the equivalent circuit in Fig. 5.

In this figure, all the rotor and power windings quantities are referred to the control-winding side. The real power P_r which is transmitted from rotor can be computed as [3] and [12]:

$$P_r = -3 \cdot \frac{E_s'^2}{\left(\frac{r_r'}{s}\right)^2 + X_{lr}'^2} \cdot \frac{r_r'}{s}. \tag{10}$$

Also, the real power which is absorbed by power windings (neglecting both the voltage drop across the linkage impedance of power windings and the copper loss of DWIG) can be written as

$$P_p = 3 \cdot \frac{E_s'^2}{R_{\mathrm{BR}}'}. \tag{11}$$

For an induction generator, of the total mechanical power delivered across the rotor to the air gap, the fraction $\frac{1}{1-s}$ is converted to electric power and the fraction $\frac{s}{s-1}$ is dissipated as $3 \cdot r_r \cdot I_r^2$ loss in the rotor conductors. Therefore

$$P_p = \frac{1}{1-s} \cdot P_r. \tag{12}$$

Combining (11) and (12) gives

$$P_r = 3 \cdot \frac{E_s'^2}{R_{\mathrm{BR}}'} \cdot (1-s). \tag{13}$$

Equation (10) can be simplified into

$$P_r . X_{lr}'^2 \cdot s^2 + 3 \cdot E_s'^2 \cdot s \cdot r_r' + P_r \cdot r_r'^2 = 0. \tag{14}$$

The slip s can be consequently derived from (8)

$$s = \frac{-3 \cdot r_r' \cdot E_s'^2 + \sqrt{9 \cdot r_r'^2 \cdot E_s'^4 - 4 \cdot X_{lr}'^2 . r_r'^2 . P_r^2}}{2 \cdot P_r \cdot X_{lr}'^2}. \tag{15}$$

Substituting (13) into (15) gives

$$s = \frac{-3 \cdot r_r' \cdot E_s^2 + 3 \cdot r_r' \cdot E_s'^2 \sqrt{1 - 4 \cdot X_{lr}'^2 \cdot \frac{(1-s)^2}{R_{\mathrm{BR}}'^2}}}{6 \cdot \frac{E_s'^2}{R_{\mathrm{BR}}'} \cdot (1-s) \cdot X_{lr}'^2}. \tag{16}$$

Equation (16) simplifies to

$$s = \frac{r_r' \cdot R_{\mathrm{BR}}'}{2 \cdot (1-s) \cdot X_{lr}'^2} \cdot \left[-1 + \sqrt{1 - 4 \cdot X_{lr}'^2 \cdot \frac{(1-s)^2}{R_{\mathrm{BR}}'^2}} \right]. \tag{17}$$

Therefore, for stable operation of DWIG with BR, the value of R_{BR} should satisfy the following condition:

$$R_{\mathrm{BR}} \geq 2 \cdot (1-s) \cdot X_{lr}. \tag{18}$$

For any type of induction generators, the slip of generator s varies between 0 and the pull-out slip $S_{T\max}$. The $S_{T\max}$ is the slip at which the pull-out torque "maximum torque" occurs. Based on the induction machines theory, the $S_{T\max}$ corresponding to a DWIG may be approximately expressed as

$$s_{T\max} = -\frac{R_r}{X_{lp} + X_{lr}}. \tag{19}$$

During the fault, to ensure stable operation of DWIG, the value of BR R_{BR} should satisfy the following condition:

$$R_{\mathrm{BR}} \geq 2 . X_{lr} . \left(1 + \frac{R_r}{X_{lp} + X_{lr}}\right). \tag{20}$$

V. Simulation Results

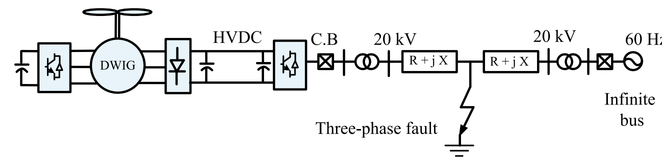

Fig. 6. Schematic diagram of the simulated system.

To evaluate the performance of the coordinated control for DWIG and BR, the model of the DWIG system with diode bridge rectifier and SEC is built up using MATLAB/Simulink. The power system configuration is presented in Fig. 6. A 15-kW DWIG is used with an output line to line rms voltage at 200 V.

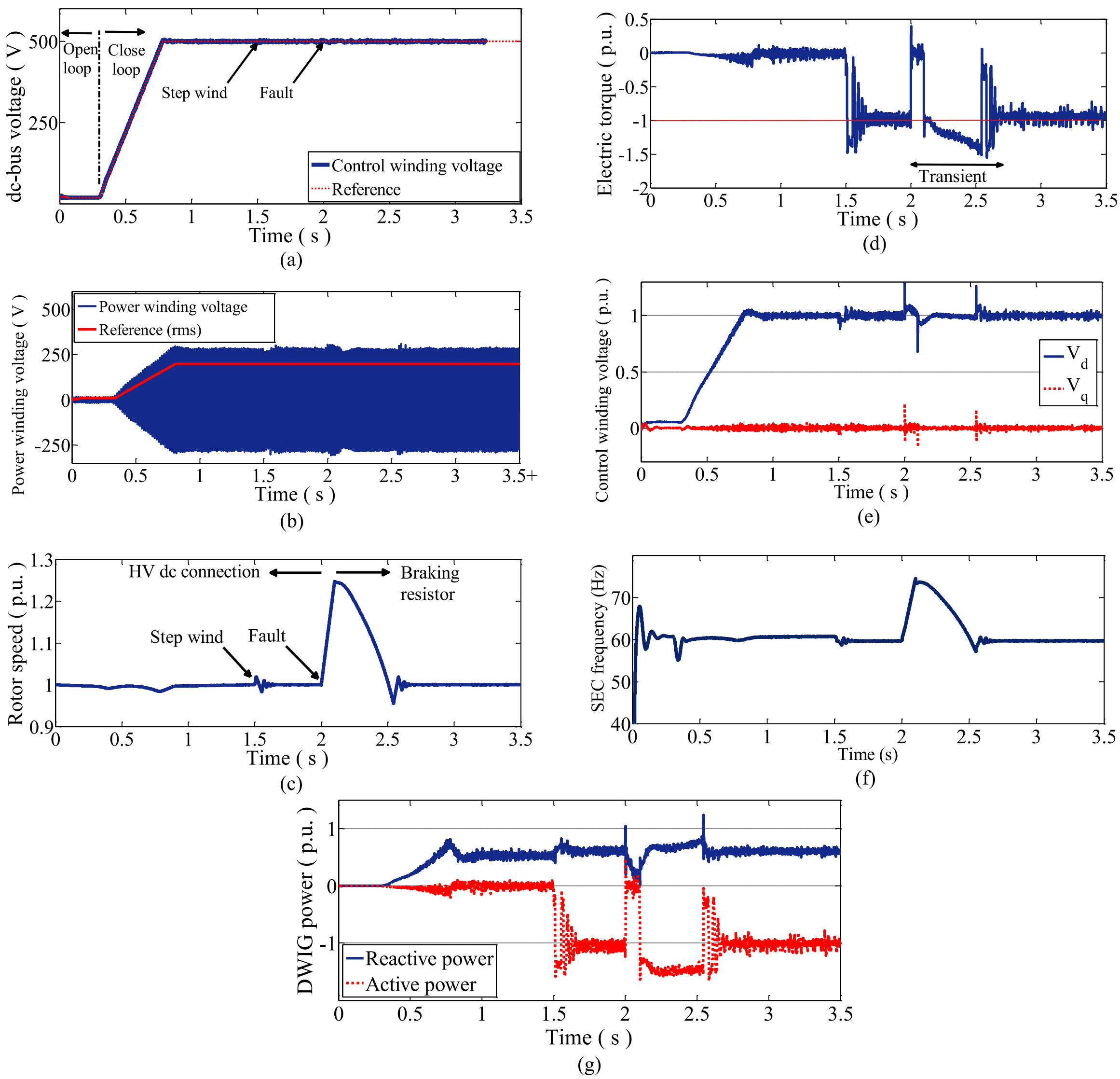

Fig. 7. Simulation results of three/three DWIG wind power system based on the proposed control strategy.

The DWIG is coupled to a HVdc transmission line via a diode bridge rectifier. The HVdc transmission is connect to a 60-Hz infinite bus via a 0.1-MVA transformer and a single-circuit ac transmission line.

In the simulated system, the parameters of 15-kW DWIG are power winding resistance is 0.01965 p.u., control winding resistance is 0.01965 p.u., rotor resistance is 0.01909 p.u., rotor and power winding inductances are 0.0397 p.u., control winding inductance is 0.0684 p.u., and mutual inductance is 1.354 p.u. L_{pr} is 0.003 p.u and L_{cr} is 0.003 p.u.

During the build-up voltage, the electric torque of DWIGs are set to -0.1 p.u. After build-up the voltage, the electric torque is stepped from -0.1 to -1 p.u at time instant 1.5 s, and the DWIGs are allowed to establish this new operating point. A solid three phase to ground fault is applied in the center of the ac line at time instant 2 s, and cleared after 0.120 s. The mechanical input torque to the DWIG is set at -1.0 p.u. throughout this study. Immediately when the fault is detected, the HVdc transmission and infinite bus are disconnected from the faulty ac transmission line by opening the circuit breakers at both ends of ac line so that the electric power of the DWIG drops to zero. At the time instant 2.12 s, the BR is connected to the power winding, and the DWIGs are allowed to establish this new operating point.

The simulation result in Fig. 7(a) shows the voltage build up, step load, prefault, and postfault of dc-bus voltage of control windings. Also, the power winding voltage of the DWIGs is illustrated in Fig. 7(b). The system begins to build up the voltage at time instant of 0.3 s with nominal rotor speed. It can be observed that $U_{c\,\mathrm{DC}}$ and $U_{p\,\mathrm{DC}}$ ramp up to 500 and 200 V, respectively, without the overshoot. Also both $U_{c\,\mathrm{DC}}$ and $U_{p\,\mathrm{DC}}$ are very well regulated during and after the sever fault. As shown in these figures, when the rated resistive load and braking resistance are added at time instant 1.5 and 2.12 s, respectively, the voltage drop and transient time are at acceptable rates [19]. Also, during the fault, the voltage fluctuation (including the voltage overshoot and voltage drop) is less than 5% of rated voltage. Therefore, during the fault, the conditions necessary for the BR to absorb maximum active power is satisfied. Also, the nominal reactive power can be generated by the fixed capacitor bank in the fault condition. Fig. 7(c) and (d) shows the rotor

Fig. 8. Experimental setup including a 1.2-kW DWIG and a 2.89-kW DC motor as a wind simulator.

speed and electric torque of DWIG, respectively. When the fault occurs at $t = 2$ s, the electrical torque drops to zero and the mechanical torque accelerates the rotor and the speed increases. The BR is connected to power winding at time $t = 2.12$ when the rotor speed has increased to 1.24 p.u. At this point, the electric torque increases from zero to 1 p.u. For $2.12 < t < 2.45$, the electrical torque is greater than mechanical torque and this acts like a braking torque reducing the speed of the rotor until once again the steady operating is reached at time instant 2.5 s. Fig. 7(e) demonstrates the *d*-axes and *q*-axes of control winding voltage. The phase-locked loop of the control system puts all the control winding voltage in the *d*-axes and after the voltage build up, the *d*-axes of control winding voltage is forced to 1 p.u. so that the *q*-axes of control winding voltage is set to zero. Fig. 7(f) also shows the frequency of the DWIG. As shown in this figure, since the control-winding voltage oriented is accomplished, the frequency of SEC follows the rotor-speed fluctuations during the disturbance. In such a situation, the slip of DWIG remains approximately constant. It is well known that the reactive power of an induction machine depends on both the slip and the terminal voltage. Hence, it can be expected that also the reactive power of the DWIG will be approximately constant. Fig. 7(g) shows the active and reactive power of the DWIG during the whole of simulation period. As shown in Fig. 7(d) and (g), although large disturbances such as step wind, fault, and BR connection cause large changes in the active power and electric torque, the reactive power of DWIG remains approximately constant.

VI. Experimental Results

Several experimental tests were conducted using a 1.2-kW DWIG to verify the effectiveness of the proposed control in improving rotor-speed stability. Some of the most important results are considered here. The measured machine parameters are presented in the appendix. The prime mover is simulated by a 2.89-kW dc machine, as shown in Fig. 8.

A DSP of TMS320F2812 is used as the controller to implement the control strategy. For the predisturbance operating condition, the power winding voltage is set to rated voltage (180-V rms phase to phase and 50-Hz frequency). The numbers of poles of the DWIG are four so that the synchronous speed of DWIG is 1500 r/min. The DC motor and DWIG operate at the rotational speed 1530 r/min with the negative slip of -0.02. The DWIG fed 0.5-kW power to the dc load via a three-phase diode bridge rectifier. At the time $t_0 = 0$, the power winding is suddenly disconnected from the dc load and the rotor speed increases from 1530 to 1830 r/min within 1 s. In this scheme, the BR consists

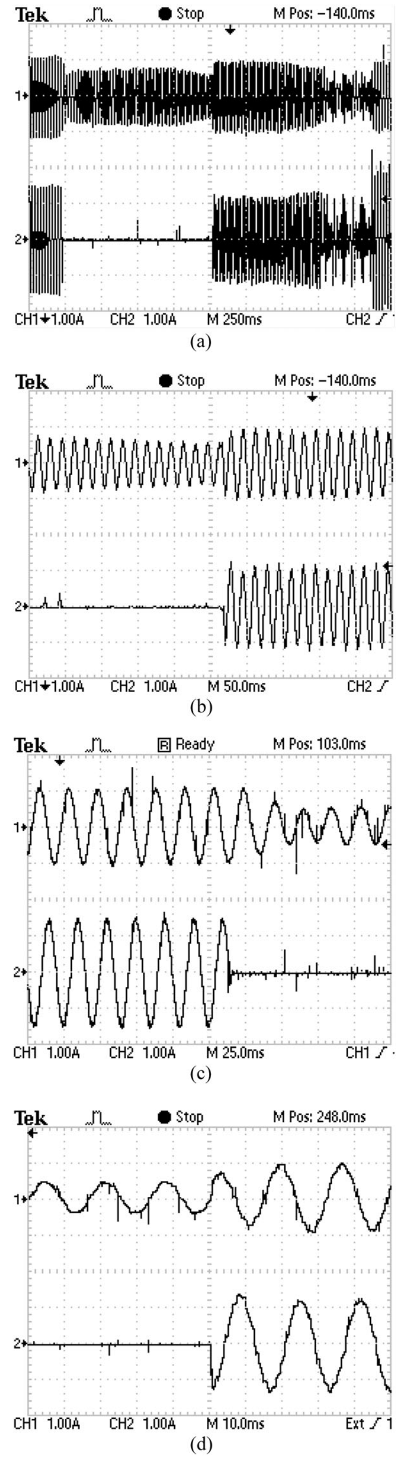

Fig. 9. Experimental results of control winding voltage oriented control (CH1. line current of control winding i_{cA}, CH2. line current of power winding i_{pA}). (a) Whole process of disturbance. (b) Experimental waveform of the transition at 1800 r/min. (c) Step unload (BR) at 1500 r/min. (d) Step load (BR) at 1800 r/min.

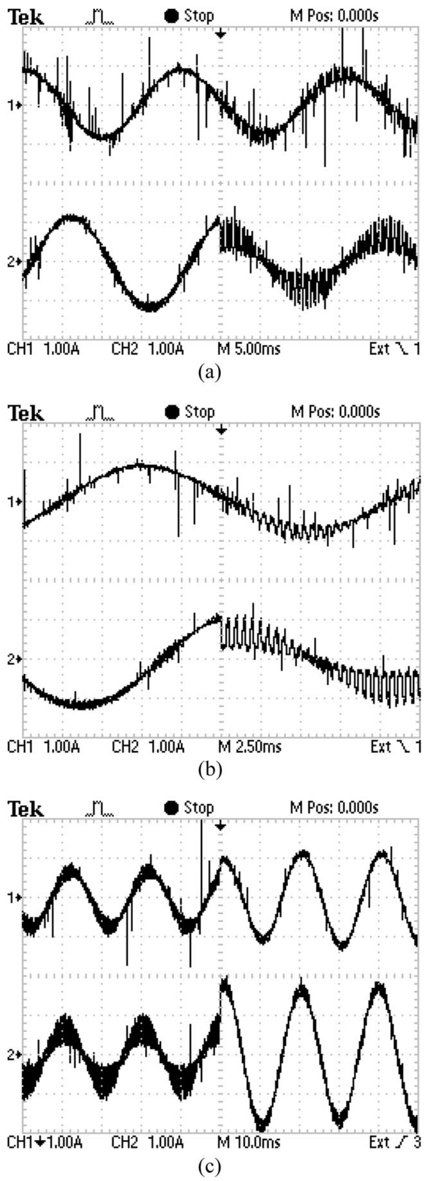

Fig. 10. (a) and (b). Experimental results of coordinate control of the DWIG and BR at the time instant 1 s. (CH1. line current of Control winding i_{cA}, CH2. line current of power winding i_{pA}). (c). Experimental results of reconnecting DC load (CH1. line current of Control winding i_{cA}, CH2. line current of power winding i_{pC}).

of a fixed 110-Ω resistance and a 220-Ω controlled resistance. The BR is connected to power winding at $t = 1s$ and the DC motor decreases the speed of DWIG to its predisturbance value within the 1.1 s at the time instant 2.1 s, the power windings are reconnected to the dc load and the BRs are disconnected at the time instant 2.1 s. Fig. 9(a) is the experiment results of control winding and power winding line current in several typical states in the whole process. This figure shows, during the disturbance ($0 < t < 2.1$), the control-winding current (reactive power consumption of DWIG) does not exceed its predisturbance value. Fig. 9(b) also shows the power- and control-winding currents during the step load (BR). According to the waves of current of the control winding, it is disclosed that control of the SEC can be achieved with the proposed control strategy. Fig. 9(c) and

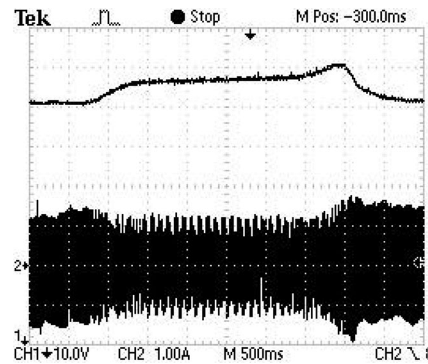

Fig. 11. Experimental results for control winding power versus rotor speed (CH1. Rotor speed, CH2. line current of control winding i_{cA}).

(d) is the experiment results of DWIG currents during the step unload (dc load) and step load (BR). During the step unload and step load, the frequency of control winding current is about 50 and 60 Hz, respectively.

As mention before, during the disturbance, the rotor speed increases from 1530 to 1830 r/min. Therefore, for a DWIG with the proposed control strategy, the synchronous speed (frequency of SEC) follows the sudden changes of the rotor speed and the slip remains approximately constant.

Fig. 10(a) and (b) shows the experimental results of line currents of DWIG under varying the load condition during the disturbance. At the time instant 1.75 s, as soon as the rotor speed reaches to it predisturbance vale, the control system increases the value of breaking resistor that prevents a further decrease in the rotor speed, thereby keeping it at 1530 r/min. Fig. 10(b) shows the currents of DWIG when the amount of BR is increased by the supplementary loop. At the time instant 1.75 s, when the rotor speed reaches to 1530 r/min, the supplementary control loop increases the value of BR by connecting the 220-Ω controlled resistance to the 110-Ω fixed resistance. This is also more clearly illustrated in Fig. 10(b).

Fig. 10(c) shows the current of phase A of control winding i_{cA} and power winding current of phase C i_{pC} of DWIG at the time instant 2.1 s. At this moment, the BR is disconnected from the power winding and the dc load can be switched ON again.

In the second test, the speed of DWIG is increased from 1530 to 1830 r/min for 3 s. This test was carried out to show that the reactive power of DWIG decreases as the rotor accelerate during the fault. Fig. 11(b) shows experimental results of the relationship between the rotor speed and the control winding current of DWIG. As shown in this figure, the control winding current (reactive power) of DWIG is approximately inversely proportional to rotor speed which is consistent with the theoretical analysis and simulation results. As mentioned earlier this feature can be taken advantage of because, during the disturbance, decreasing the reactive power consumption will result better dynamic behavior.

VII. Conclusion

In order to apply the DWIG system in the offshore wind farms, a novel control-winding voltage oriented drive is proposed in this paper. The main idea is to combine the conventional voltage oriented control with the BR so that a novel control-winding oriented drive is presented. The proposed drive strategy is tailored in order to adjust the value of BR according to the mechanical torque of the wind turbine, preventing rotor acceleration. Also, the orientation of control winding voltage forces the slip of DWIG to be approximately constant, thereby limiting the reactive power consumption during the fault. MATLAB/Simulink simulation and experimental results confirm the validity of the proposed method. As a summary of the proposed strategy advantages it can be said that: 1) the control methodology has no direct relation with machine parameters, so it is not sensitive to them, 2) the power winding voltage remains approximately constant during the fault so that the fixed capacitor generates more reactive power during the acceleration period. Also, maximum electric would be absorbed by BR, 3) the constant-slip operation of DWIG observed when the control-winding voltage oriented drive is accomplished. This causes the reactive power to be limited during the disturbance. 4) Different from synchronous generator cases, no possibility of back-swing instability has been observed if the BR is switched ON for a long time.

Appendix

The main parameters of the prototype 1.2-kW 115V DWIG system are as follows: $R_p = 0.46\,\Omega$; $R'_c = 0.91\,\Omega$; $R'_r = 0.81\,\Omega$; $L_p = 2.02\,\mathrm{mH}$; $L'_c = 4.04\,\mathrm{mH}$; $L'_r = 2.1\,\mathrm{mH}$; $L_m = 70\,\mathrm{mH}$; $L_{lpc} = 2\,\mathrm{mH}$; dc-bus voltage of SEC = 270 V; voltage of battery 48 V, dc-bus capacitor = 0.560 mF; Numbers of poles = 4.

References

[1] S. M. Muyeen, R. Takahashi, and J. Tamura, "Operation and control of HVDC-connected offshore wind farm," *IEEE Trans. Sustainable Energy*, vol. 1, no. 1, pp. 30–37, Apr. 2010.

[2] R. E. Torres-Olguin, M. Molinas, and T. Undeland, "Offshore wind farm grid integration by VSC technology with LCC-based HVDC transmission," *IEEE Trans. Sustainable Energy*, vol. 3, no. 4, pp. 899–907, Oct. 2012.

[3] F. Bu, W. Huang, Y. Hu, and K. Shi, "An excitation-capacitor-optimized dual stator-winding induction generator with the static excitation controller for wind power application," *IEEE Trans. Energy Convers.*, vol. 26, no. 1, pp. 122–131, Mar. 2011.

[4] Z. Wu, O. Ojo, and J. Sastry, "High-performance control of a dual stator winding DC power induction generator," *IEEE Trans. Ind. Appl.*, vol. 43, no. 2, pp. 582–592, Mar./Apr. 2007.

[5] F. Bu, W. Huang, Y. Hu, and S. Zhuang, "Parameter design and static performance of dual stator-winding induction generator variable frequency AC generating system with inductive and capacitive loads," *IEEE Trans. Ind. Electron.*, vol. 61, no. 8, pp. 3902–3914, Aug. 2014.

[6] O. Ojo and I. E. Davidson, "PWM-VSI inverter-assisted stand-alone dual stator winding induction generator," *IEEE Trans. Ind. Appl.*, vol. 36, no. 6, pp. 1604–1611, Nov./Dec. 2000.

[7] F. Bu, W. Huang, Y. Hu, S. Zhuang, and K. Shi, "Wide-speed-range-operation dual stator-winding induction generator DC generating system for wind power applications," *IEEE Trans. Power Electron.*, vol. 30, no. 2, pp. 561–573, Feb. 2015.

[8] M. H. Zamani, S. H. Fathi, G. H. Riahy, M. Abedi, and N. Abdolghani, "Improving transient stability of grid-connected squirrel-cage induction generators by plugging mode operation," *IEEE Trans. Energy Conver.*, vol. 27, no. 3, pp. 707–714, Sep. 2012.

[9] L. Xu, L. Yao, and C. Sasse, "Comparison of using SVC and STATCOM for wind farm integration," in *Proc. Int. Conf. Power Syst. Technol.*, Oct. 22–26, 2006, pp. 1–7.

[10] D. Wang, W. Ma, F. Xiao, B. Zhang, D. Liu, and A. Hu, "A novel stand-alone dual stator-winding induction generator with static excitation regulation," *IEEE Trans. Energy Conver.*, vol. 20, no. 4, pp. 826–835, Dec. 2005.

[11] W. Freitas, A. Morelato, and X. Wilsun, "Improvement of induction generator stability using braking resistors," *IEEE Trans. Power Syst.*, vol. 19, no. 2, pp. 1247–1249, May 2004.

[12] Y. Li, Y. Hu, W. Huang, L. Liu, and Z. Yong, "The capacity optimization for the static excitation controller of the dual-stator-winding induction generator operating in a wide speed range," *IEEE Trans. Ind. Electron.*, vol. 56, no. 2, pp. 530–541, Feb. 2009.

[13] S. M. Muyeen, H. M. Hasanien, and A. Al-Durra, "Transient stability enhancement of wind farms connected to a multi-machine power system by using an adaptive ANN-controlled SMES," *Energy Convers. Manage.*, vol. 78, pp. 412–420, 2014.

[14] R. Patel, T. S. Bhatti, and D. P. Kothari, "Improvement of power system transient stability by coordinated operation of fast valving and braking resistor," *IEE Proc-Gener. Trans. Distrib.*, vol. 150, no. 3, pp. 311–316, May 2003.

[15] P. C. Krauce, O. Wasynczuk, and S. D. Suddhof, *Analysis of Electric Machinery and Drive Systems*, 2nd ed. New York, NY, USA: Wiley, 2002.

[16] K. Shi, W. Huang, Y. Hu, and F. Bu, "An indirect-field-oriented dual stator-winding induction generator for the wind power system applications," in *Proc. World Non-Grid-Connected Wind Power Energy Conf.*, Sep. 24–26, 2009, pp. 1–5.

[17] H. Yuwen, H. Wenxin, and L. Yong, "A novel instantaneous torque control scheme for induction generator systems," *IEEE Trans. Energy Conver.*, vol. 25, no. 3, pp. 463–471, Sep. 2010.

[18] J. Machowski, J. W. Bialek, and J. R. Bumby, *Power System Dynamics: Stability and Control*, 2nd ed. New York, NY, USA: Wiley, 2008.

[19] F. Bu, W. Huang, Y. Hu, S. Zhuang, and K. Shi, "Control strategy and dynamic performance of dual stator-winding induction generator variable frequency AC generating system with inductive and capacitive loads," *IEEE Trans. Power Electron.*, vol. 29, no. 4, pp. 1681–1692, Apr. 2014.

Mohammad Hassan Zamani received the B.Sc. degree in electrical engineering from Islamic Azad University, Najafabad, Iran, in 2001, and the M.Sc. degree from the Amirkabir University of Technology, Tehran, Iran, where he is currently working toward the Ph.D. degree in the Wind Energy Lab.

His research interests include wind power generation and induction machines.

Gholam hossein Riahy received the B.Sc. and M.Sc. degrees from the Amirkabir University of Technology, Tehran, Iran, in 1989 and 1993, respectively, and the Ph.D. degree from Monash University, Melbourne, Vic., Australia, in 1999.

He was with the Amirkabir University of Technology in 2000, and he is currently a Member of Center of Excellency on Power Systems. His main research interest includes renewable energy systems.

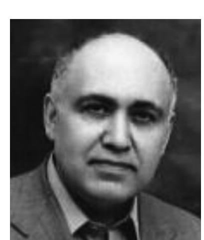

Mehrdad Abedi received the B.Sc. degree from Tehran University, Tehran, Iran, the M.Sc. degree from London University, London, England, U.K., and the Ph.D. degree from Newcastle University, England, in 1970, 1973, and 1977, respectively.

He was with the General Electric Company, England, until 1978. Since then he was with the Department of Electrical Engineering, Amirkabir University, Tehran, Iran, where he is currently a Professor and the Head of the Center of Excellence on power system. He has published more than 30 books and 180 papers in journals and conferences. He is a Distinguished Professor in Iran and is prize winner for two outstanding books. He is also a Member of Iranian Academy of Science and Member of CIGRE. His main research interests include electrical machines and power systems modeling, operation and control.